Eur. Phys. J. D **46**, 335–344 (2008)
DOI: 10.1140/epjd/e2007-00291-5

THE EUROPEAN PHYSICAL JOURNAL D

Geometric phase of a qubit interacting with a squeezed-thermal bath

S. Banerjee[1] and R. Srikanth[2,1,a]

[1] Raman Research Institute, Sadashiva Nagar, Bangalore 560 080, India
[2] Poornaprajna Institute of Scientific Research, Devanahalli, Bangalore 562 110, India

Received 4 July 2007 / Received in final form 5 September 2007
Published online 17 October 2007 –

Abstract. We study the geometric phase of an open two-level quantum system under the influence of a squeezed, thermal environment for both non-dissipative as well as dissipative system-environment interactions. In the non-dissipative case, squeezing is found to have a similar influence as temperature, of suppressing geometric phase, while in the dissipative case, squeezing tends to counteract the suppressive influence of temperature in certain regimes. Thus, an interesting feature that emerges from our work is the contrast in the interplay between squeezing and thermal effects in non-dissipative and dissipative interactions. This can be useful for the practical implementation of geometric quantum information processing. By interpreting the open quantum effects as noisy channels, we make the connection between geometric phase and quantum noise processes familiar from quantum information theory.

PACS. 03.65.Vf Phases: geometric; dynamic or topological – 03.65.Yz Decoherence; open systems; quantum statistical methods – 03.67.Lx Quantum computation

1 Introduction

Geometric Phase (GP) brings about an interesting and important connection between phase and the intrinsic curvature of the underlying Hilbert space. In the classical context it was introduced by Pancharatnam [1], who defined a phase characterizing the interference of classical light in distinct states of polarization. Its quantum counterpart was discovered by Berry [2] for the case of cyclic adiabatic evolution. Simon [3] showed this to be a consequence of the holonomy in a line bundle over parameter space thus establishing the geometric nature of the phase. Generalization of Berry's work to non-adibatic evolution was carried out by Aharonov and Anandan [4] and to the case of non-cyclic evolution by Samuel and Bhandari [5], who by extending Pancharatnam's ideas for the interference of polarized light to quantum mechanics were able to make a comparison of the phase between any two non-orthogonal vectors in the Hilbert space. An important development was carried out by Mukunda and Simon [6], who, making use of the fact that GP is a consequence of quantum kinematics, and is thus independent of the detailed nature of the dynamics in state space, formulated a quantum kinematic version of GP.

Uhlmann was the first to extend GP to the case of nonunitary evolution of mixed states, employing the standard purification of mixed states [7]. Sjöqvist et al. [8] introduced an alternate definition of geometric phase for nondegenerate density operators undergoing unitary evolution, which was extended by Singh et al. [9] to the case of degenerate density operators. A kinematic approach to define GP in mixed states undergoing nonunitary evolution, generalizing the results of the above two works, has recently been proposed by Tong et al. [10]. Wang et al. [11,12] defined a GP based on a mapping connecting density matrices representing an open quantum system, with a nonunit vector ray in complex projective Hilbert space, and applied it to study the effects of a squeezed-vacuum reservoir on GP.

The geometric nature of GP provides an inherent fault tolerance that makes it a useful resource for use in devices such as a quantum computer [13]. There have been proposals to observe GP in a Bose-Einstein-Josephson junction [14] and in a superconducting nanostructure [15], and of using it to control the evolution of the quantum state [16]. However, in these situations the effect of the environment is never negligible [17]. Also in the context of quantum computation, the qubits are never isolated but under some environmental influence. Hence it is imperative to study GP in the context of Open Quantum Systems. An important step in this direction was taken by Whitney et al. [18], who carried out an analysis of the Berry phase in a dissipative environment [19]. Rezakhani and Zanardi [20] and Lombardo and Villar [21] have also carried out an open system analysis of GP, where they were concerned, amongst other things, with the interplay

[a] e-mail: srik@rri.res.in

between decoherence and GP brought about by thermal effects from the environment. Sarandy and Lidar [22] have introduced a self-consistent framework for the analysis of Abelian and non-Abelian geometric phases for open quantum systems undergoing cyclic adiabatic evolution. The GP acquired by open bipartite systems has recently been studied by Yi et al. [23] using the quantum trajectory approach.

In this paper we make use of the method of Tong et al. [10] to study the GP of a qubit (a two-level quantum system) interacting with different kinds of system-bath (environment) interactions, one in which there is no energy exchange between the system and its environment, i.e., a quantum non-demolition (QND) interaction and one in which dissipation takes place [24,25]. Throughout, we assume the bath to start in a squeezed thermal initial state, i.e., we deal with a squeezed thermal bath. The physical significance of squeezed thermal bath is that the decay rate of quantum coherences in phase-sensitive (i.e., squeezed) baths can be significantly modified compared to the decay rate in ordinary (phase-insensitive) thermal baths [26–28]. A method to generate GP by making use of a squeezed vacuum bath has recently been proposed by Carollo et al. [29].

The open system effects studied below can be given an operator-sum or Kraus representation [30]. In this representation, a superoperator $\mathcal{E}$ due to environmental interaction, acting on the state of the system is given by

$$\rho \longrightarrow \mathcal{E}(\rho) = \sum_k \langle e_k|U(\rho \otimes |f_0\rangle\langle f_0|)U^\dagger|e_k\rangle = \sum_j E_j \rho E_j^\dagger, \tag{1}$$

where U is the unitary operator representing the free evolution of the system, reservoir, as well as the interaction between the two, $\{|f_0\rangle\}$ is the environment's initial state, and $\{|e_k\rangle\}$ is a basis for the environment. The environment and the system are assumed to start in a separable state. In the above equation, $E_j \equiv \langle e_k|U|f_0\rangle$ are the Kraus operators, which satisfy the completeness condition $\sum_j E_j^\dagger E_j = \mathcal{I}$. The operator sum representation is not unique. Every (infinitely many) possible choice of tracing basis $\{|e_k\rangle\}$ in equation (1) yields a different, but equivalent and unitarily related, set of Kraus operators. It can be shown that any transformation that can be cast in the form (1) is a completely positive (CP) map [31].

From the viewpoint of quantum communication, these open quantum system effects correspond to noisy quantum channels, and are recast in the Kraus representation. We find that some of them may be interpreted in terms of familiar noisy quantum channels. This abstraction will enable us to connect noisy channels directly to their effect on GP, bypassing system-specific details. Visualizing the effect of these channels on GP in a Bloch vector picture of these open system effects helps to interpret our GP results in a simple fashion.

The structure of the paper is as follows. In Section 2, we briefly discuss QND open quantum systems and collect some formulas which would be of use later. In Section 3, we study the GP of a two-level system in QND interaction with its bath. Here we consider two different kinds of baths. In Section 3.1, a bath of harmonic oscillators is considered, and we also briefly touch upon a bath of two-level systems. In Section 3.2, we point out that the GP results obtained in this section are generic for any purely dephasing channel. In Section 4, we study the GP of a two-level system in a dissipative bath. Section 4.1 considers the system interacting with a bath of harmonic oscillators in the weak Born-Markov, rotating-wave approximation (RWA). In Section 4.2, we point out that the GP results obtained in this section are generic for any squeezed generalized amplitude damping channel [32], of which the familiar generalized amplitude damping channel [31] is a special case. We make our conclusions in Section 5.

2 QND open quantum systems – A recapitulation

To illustrate the concept of QND open quantum systems we use the percept of a system interacting with a bath of harmonic oscillators. Such a model, for a two-level atom, has been studied [33–35] in the context of influence of decoherence in quantum computation. We will consider the following Hamiltonian which models the interaction of a system with its environment, modelled as a bath of harmonic oscillators, via a QND type of coupling [28]

$$\begin{aligned} H &= H_S + H_R + H_{SR} \\ &= H_S + \sum_k \hbar\omega_k b_k^\dagger b_k + H_S \sum_k g_k (b_k + b_k^\dagger) \\ &\quad + H_S^2 \sum_k \frac{g_k^2}{\hbar\omega_k}. \end{aligned} \tag{2}$$

Here H_S, H_R and H_{SR} stand for the Hamiltonians of the system (S), reservoir (R) and system-reservoir (S-R) interaction, respectively. The last term on the right-hand side of equation (1) is a renormalization inducing 'counter term'. Since $[H_S, H_{SR}] = 0$, (1) is of QND type. Here H_S is a generic system Hamiltonian which we will use in the subsequent sections to model different physical situations. The system plus reservoir complex is closed obeying a unitary evolution given by

$$\rho(t) = e^{-\frac{i}{\hbar}Ht}\rho(0)e^{\frac{i}{\hbar}Ht}, \tag{3}$$

where $\rho(0) = \rho^s(0)\rho_R(0)$, i.e., we assume separable initial conditions. Here we assume the reservoir to be initially in a squeezed thermal state, i.e., a squeezed thermal bath, with an initial density matrix $\rho_R(0)$ given by

$$\rho_R(0) = S(r,\Phi)\rho_{\rm th}S^\dagger(r,\Phi), \tag{4}$$

where $\rho_{\rm th} = \prod_k \left[1 - e^{-\beta\hbar\omega_k}\right] \exp\left(-\beta\hbar\omega_k b_k^\dagger b_k\right)$ is the density matrix of the thermal bath, and

$$S(r_k,\Phi_k) = \exp\left[r_k\left(\frac{b_k^2}{2}e^{-i2\Phi_k} - \frac{b_k^{\dagger 2}}{2}e^{i2\Phi_k}\right)\right]$$

is the squeezing operator with r_k, Φ_k being the squeezing parameters [36]. In an open system analysis we are interested in the reduced dynamics of the system of interest S which is obtained by tracing over the bath degrees of freedom. Using equations (2) and (3) and tracing over the bath we obtain the reduced density matrix for S, in the system eigenbasis, as [28]

$$\rho^s_{nm}(t) = e^{-\frac{i}{\hbar}(E_n-E_m)t} e^{i(E_n^2-E_m^2)\eta(t)} e^{-(E_n-E_m)^2\gamma(t)} \rho^s_{nm}(0). \quad (5)$$

Here

$$\eta(t) = -\sum_k \frac{g_k^2}{\hbar^2\omega_k^2}\sin(\omega_k t), \quad (6)$$

and

$$\gamma(t) = \frac{1}{2}\sum_k \frac{g_k^2}{\hbar^2\omega_k^2}\coth\left(\frac{\beta\hbar\omega_k}{2}\right)\big|(e^{i\omega_k t}-1)\cosh(r_k) + (e^{-i\omega_k t}-1)\sinh(r_k)e^{i2\Phi_k}\big|^2. \quad (7)$$

For the case of an Ohmic bath with spectral density $I(\omega) = \frac{\gamma_0}{\pi}\omega e^{-\omega/\omega_c}$, where γ_0 and ω_c are two bath parameters, $\eta(t)$ and $\gamma(t)$ have been evaluated in [28], where we have for simplicity taken the squeezed bath parameters as

$$\cosh(2r(\omega)) = \cosh(2r), \quad \sinh(2r(\omega)) = \sinh(2r), \quad \Phi(\omega) = a\omega,$$

with a being a constant depending upon the squeezed bath. We will make use of equations (6) and (7) in the subsequent analysis (cf. Ref. [28] for details). Note that the results pertaining to a thermal bath can be obtained from the above equations by setting the squeezing parameters r and Φ (i.e., a) to zero.

3 GP of two-level system in QND interaction with bath

In this section we study the GP of a two-level system in QND interaction with its environment (bath). We consider two classes of baths, one being the commonly used bath of harmonic oscillators [21], and the other being a localized bath of two-level systems.

3.1 Bath of harmonic oscillators

The total Hamiltonian of the $S+R$ complex has the same form as in equation (2) with the system Hamiltonian $H_S = \frac{\hbar\omega}{2}\sigma_3$, where σ_3 is the usual Pauli matrix. We will be interested in obtaining the reduced dynamics of the system. This is done by studying the reduced density matrix of the system whose structure in the system eigenbasis is as in equation (5). For the system described by H_S an appropriate eigenbasis is given by the Wigner-Dicke states [37–39] $|j,m\rangle$, which are the simultaneous eigenstates of the angular momentum operators J^2 and J_Z, and we have $H_S|j,m\rangle = \hbar\omega m|j,m\rangle = E_{j,m}|j,m\rangle$. Here $-j \le m \le j$. For the two-level system considered here, $j = \frac{1}{2}$ and hence $m = -\frac{1}{2}, \frac{1}{2}$. Using this basis in equation (5) we obtain the reduced density matrix of the system as

$$\rho^s_{jm,jn}(t) = e^{-i\omega(m-n)t} e^{i(\hbar\omega)^2(m^2-n^2)\eta(t)} \times e^{-(\hbar\omega)^2(m-n)^2\gamma(t)} \rho^s_{jm,jn}(0). \quad (8)$$

It follows from equation (8) that the diagonal elements of the reduced density matrix signifying the population remain unaffected by the environment whereas the off-diagonal elements decay. This is a feature of the QND nature of the system-environment coupling. Initially we choose the system to be in the state

$$|\psi(0)\rangle = \cos\left(\frac{\theta_0}{2}\right)|1\rangle + e^{i\phi_0}\sin\left(\frac{\theta_0}{2}\right)|0\rangle. \quad (9)$$

Using this we can write equation (8) as

$$\begin{aligned}
\rho^s_{j0,j0}(t) &= \cos^2\left(\frac{\theta_0}{2}\right) \\
\rho^s_{j0,j1}(t) &= \frac{1}{2}\sin(\theta_0)e^{-i(\omega t+\phi_0)}e^{-(\hbar\omega)^2\gamma(t)} \\
\rho^s_{j1,j0}(t) &= \frac{1}{2}\sin(\theta_0)e^{i(\omega t+\phi_0)}e^{-(\hbar\omega)^2\gamma(t)} \\
\rho^s_{j1,j1}(t) &= \sin^2\left(\frac{\theta_0}{2}\right).
\end{aligned} \quad (10)$$

We will make use of equation (10) to obtain the GP of the above open system using the prescription of Tong et al. [10]

$$\Phi_{\rm GP} = \arg\left(\sum_{k=1}^N \sqrt{\lambda_k(0)\lambda_k(\tau)}\langle\Psi_k(0)|\Psi_k(\tau)\rangle \times e^{-\int_0^\tau dt\langle\Psi_k(t)|\dot{\Psi}_k(t)\rangle}\right). \quad (11)$$

Hereafter we will consider for GP a quasi-cyclic path where time (t) varies from 0 to $\tau = 2\pi/\omega$, ω being the system frequency. In the above equation the overhead dot refers to derivative with respect to time and $\lambda_k(\tau)$, $\Psi_k(\tau)$ refer to the eigenvalues and the corresponding eigenvectors, respectively, of the reduced density matrix given here by equation (10). The eigenvalues of equation (10) are

$$\lambda_\pm(t) = \frac{1}{2}\left[1 + \cos(\theta_0)\epsilon_\pm(t)\right], \quad (12)$$

where $\epsilon_\pm(t) = \pm\sqrt{1+\tan^2(\theta_0)e^{-2(\hbar\omega)^2\gamma(t)}}$. Since $\gamma(t) = 0$ for $t = 0$, we can see from the above equations that $\lambda_+(0) = 1$ and $\lambda_-(0) = 0$. From the structure of equation (11) we see that only the eigenvalue λ_+ and its corresponding eigenvector $|\Psi_+\rangle$ need be considered for the GP. This normalized eigenvector is found to be

$$|\Psi_+(t)\rangle = \sin\left(\frac{\theta_t}{2}\right)|1\rangle + e^{i(\omega t+\phi_0)}\cos\left(\frac{\theta_t}{2}\right)|0\rangle, \quad (13)$$

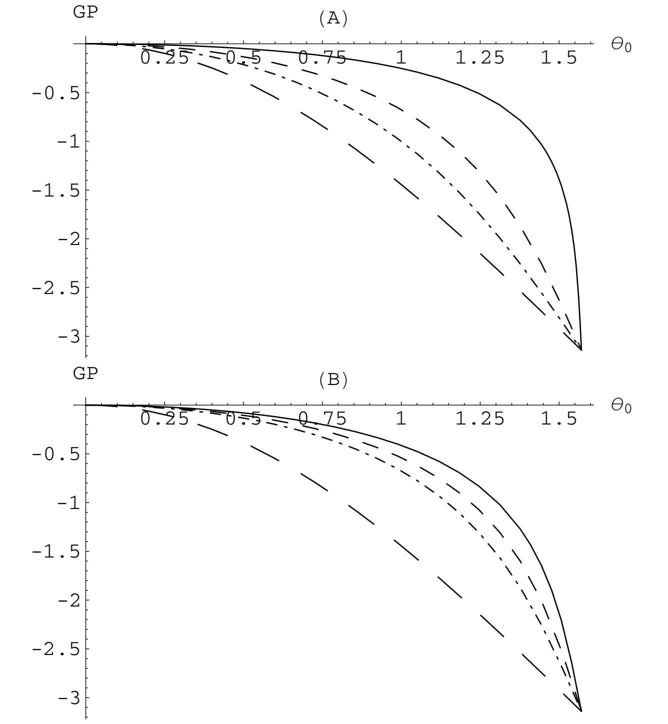

Fig. 1. GP (Eq. (14)) as a function of θ_0 (in radians) for different temperatures and squeezing at $\gamma_0 = 0.0025$. In both plots, unitary evolution is depicted by the large-dashed curve. (A) GP at $r = a = 0.0$; the dot-dashed, small-dashed and solid curves correspond, respectively, to temperatures 50, 100, 300. (B) GP at $T = 100$ and $a = 0$; the dot-dashed, small-dashed and solid curves correspond, respectively, to squeezing parameter $r = 0$, 0.4, 0.6. For QND interactions, in the region $\pi/2 < \theta_0 \leq \pi$, the pattern is symmetric but sign reversed. Observe that, as is true for all QND cases, GP vanishes at $\theta_0 = 0$. This can be attributed to the fact that the qubit's evolution sweeps no solid angle in this case. Here, as in all other figures, we take $\omega = 1$, and for all figures in this section, $\omega_c = 40\omega$.

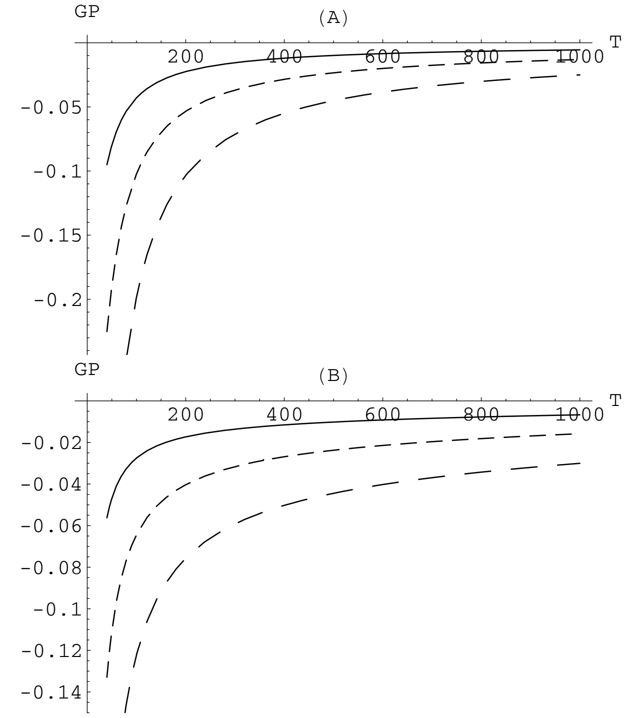

Fig. 2. GP (in radians) as a function of temperature (T, in units where $\hbar \equiv k_B \equiv 1$) for QND interaction with a bath of harmonic oscillators (Eq. (14)). (A) with $\gamma_0 = 0.005$ and vanishing squeezing. The solid, dashed and larger-dashed lines correspond to $\theta_0 = \pi/8, 3\pi/16$ and $\pi/4$. (B) Same as (A), except that here squeezing is non-vanishing, with $r = 0.7$ and $a = 0.1$.

where $\sin(\theta_t/2) = \sqrt{\frac{\epsilon_+ + 1}{2\epsilon_+}}$. It can be seen that for $t = 0$, $\sin\left(\frac{\theta_t}{2}\right) \to \cos\left(\frac{\theta_0}{2}\right)$ and $\cos\left(\frac{\theta_t}{2}\right) \to \sin\left(\frac{\theta_0}{2}\right)$, as expected. Now we make use of equations (12) and (13) in equation (11) to obtain GP as

$$\begin{aligned}\Phi_{\rm GP} = \arg\Bigg[&\left\{\frac{1}{2}\left(1+\cos(\theta_0)\sqrt{1+\tan^2(\theta_0)e^{-2(\hbar\omega)^2\gamma(\tau)}}\right)\right\}^{\frac{1}{2}} \\ &\times\left\{\cos(\frac{\theta_0}{2})\sin\left(\frac{\theta_\tau}{2}\right) + e^{i\omega\tau}\sin\left(\frac{\theta_0}{2}\right)\cos(\frac{\theta_\tau}{2})\right\} \\ &\times e^{-i\omega\int_0^\tau dt\cos^2(\frac{\theta_t}{2})}\Bigg]. \end{aligned} \quad (14)$$

Here $\gamma(t)$ is as given in reference [28] for a zero temperature (T) bath or high T bath. It can be easily seen from equation (14) that if we set the influence of the environment, encapsulated here by the expression $\gamma(t)$, to zero, we obtain for $\tau = \frac{2\pi}{\omega}$, $\Phi_{GP} = -\Omega/2 = -\pi(1 - \cos(\theta_0))$, where Ω is solid angle subtended by the tip of the Bloch vector on the Bloch sphere, which is the standard result for the unitary evolution of an initial pure state. More generally, unitary evolution of mixed states also has a simple relation to the solid angle, given by

$$\Phi_{\rm GP} = -\tan^{-1}\left(L\tan\frac{\Omega}{2}\right), \quad (15)$$

where L is the length of the Bloch vector [8,9].

The effect of temperature and squeezing on GP is brought out by Figures 1 and 2. From Figures 1A and 1B, we see, respectively, that increasing the temperature and squeezing induce a departure from unitary behavior by suppressing GP, except at polar angles $\theta_0 = 0, \pi/2$ of the Bloch sphere. It can be shown that, similarly, increase in the S-R coupling strength, modelled by γ_0, also tends to suppress GP. (Throughout this article, the figures use $\omega = 1$. Further, figures in this section use $\omega_c = 40\omega$.) The suppressive influence of temperature on GP is also seen in Figure 2, where temperature is varied for fixed θ_0 and squeezing. A similar suppressive influence of squeezing on GP is brought out by comparing Figures 2A and 2B. These observations are easily interpreted in the Bloch vector picture, as we discuss later in this section.

Another interesting case is that of qubit subjected to a bath of two-level systems, studied by Shao and collaborators in the context of QND systems [40], and quantum computation [41]. It has also been used to model a nanomagnet coupled to nuclear and paramagnetic spins [42]. It can be shown [43] that this case is mathematically similar to that of QND interaction with a vacuum bath of harmonic oscillators for weak S-R coupling, and hence the dependence of GP on θ_0 and γ_0 is similar to the analogous case discussed above.

3.2 Evolution of GP in a phase damping channel

While the results derived above are for QND S-R interactions with two types of baths, they are quite general, and in fact apply to any open system effect that can be characterized as a phase damping channel [31]. This is a uniquely non-classical quantum mechanical noise process, describing the loss of quantum information without the loss of energy. This system can be represented by the Kraus operator elements

$$E_0 \equiv \begin{bmatrix} 1 & 0 \\ 0 & e^{i\beta(t)}\sqrt{1-\lambda(t)} \end{bmatrix}, \quad E_1 \equiv \begin{bmatrix} 0 & 0 \\ 0 & \sqrt{\lambda(t)} \end{bmatrix}, \quad (16)$$

where $\beta(t)$ encodes the free evolution of the system and $\lambda(t)$ the effect of the environment. It is not difficult to see that the QND interactions we have considered realize a phase damping channel.

In the case of QND interaction with a bath of harmonic oscillators (Sect. 3.1), it is straightforward to verify that with the identification

$$\lambda(t) = 1 - \exp\left[-2(\hbar\omega)^2\gamma(t)\right]; \qquad \beta(t) = \omega t. \quad (17)$$

The operators (16) acting on the state (9) reproduce the evolution equation (10) by means of the map equation (1). Similarly, the effect of QND interaction with a bath of two level systems can also be represented as phase damping channel [43]. Our result is in agreement with that of reference [11], where GP is shown to depend on the dephasing parameter, introduced phenomenologically. Our result is obtained from a microscopic model, governed by equations (2)–(4), that takes into consideration the interaction of a qubit with a squeezed thermal bath, the resulting dynamics being shown above to be equivalent to a phase damping channel.

In the case of QND interaction, any initial state not located on the σ_3-axis tends to inspiral towards it, its trajectory remaining coplanar on the x-y plane. Consequently, the entire Bloch sphere shrinks into a prolate spheroid, with its axis of symmetry given by the σ_3-axis. The extent of inspiral depends upon the parameter $\lambda(t)$; the greater is $\lambda(t)$, the more is the inspiral. Greater squeezing and higher temperature accentuate this shrinking.

Guided qualitatively by the relation equation (15) we may interpret GP as directly dependent on the Bloch vector length $L(t)$, and the solid angle (Ω) subtended at the center of the Bloch sphere during a cycle in parameter space. Increasing T, γ_0 or squeezing results in a larger degree of inspiral causing a reduction of both L and Ω, and hence greater suppression of GP relative to the case of unitary evolution.

In Figures 1A and 1B, we noted that the GP remains invariant at polar angles $\theta_0 = 0$ and $\theta_0 = \pi/2$. In the case $\theta_0 = 0$, the Bloch vector remains a constant $(0, 0, 1)$ throughout the evolution and hence accumulates no GP. In the case $\theta_0 = \pi/2$, note that $\Omega = 2\pi$. From equation (15), we see that irrespective of the length of the Bloch vector, GP should remain the same, i.e., $-\pi$. This suggests that in the general nonunitary case, when the Bloch vector rotates on the equitorial plane, GP is unaffected by whether or not there is an inspiral of the Bloch vector.

The fall of GP as a function of T (Figs. 1A and 2) can be attributed to the fact that as T increases the tip of the Bloch vector inspirals more rapidly towards the σ_3-axis, and thus sweeps less GP. Squeezing has the same effect as temperature, of contracting the Bloch sphere along the σ_3-axis, leading to further suppression of GP (Figs. 1B and 2B).

4 GP of two-level system in non-QND interaction with bath

In this section we study the GP of a two-level system in a non-QND interaction with its bath which we take as one composed of harmonic oscillators. We consider the case of the system interacting with a bath which is initially in a squeezed thermal state, in the weak coupling Born-Markov RWA.

4.1 System interacting with bath in the weak Born-Markov RWA

Now we take up the case of a two-level system interacting with a squeezed thermal bath in the weak Born-Markov, rotating wave approximation. This kind of system-reservoir (S–R) interaction is consonant with the realization that in order to be able to observe GP, one should be in a regime where decoherence is not predominant [18,20]. The system Hamiltonian is H_S and it interacts with the bath of harmonic oscillators via the atomic dipole operator which in the interaction picture is given as

$$\mathbf{D}(t) = \mathbf{d}\sigma_- e^{-i\omega t} + \mathbf{d}^*\sigma_+ e^{i\omega t}, \quad (18)$$

where $\mathbf{d}$ is the transition matrix elements of the dipole operator. The evolution of the reduced density matrix operator of the system S in the interaction picture has the following form [44,45]

$$\begin{aligned} \frac{d}{dt}\rho^s(t) &= \gamma_0(N+1) \\ &\times \left(\sigma_-\rho^s(t)\sigma_+ - \frac{1}{2}\sigma_+\sigma_-\rho^s(t) - \frac{1}{2}\rho^s(t)\sigma_+\sigma_-\right) \\ &+\gamma_0 N\left(\sigma_+\rho^s(t)\sigma_- - \frac{1}{2}\sigma_-\sigma_+\rho^s(t) - \frac{1}{2}\rho^s(t)\sigma_-\sigma_+\right) \\ &-\gamma_0 M\sigma_+\rho^s(t)\sigma_+ - \gamma_0 M^*\sigma_-\rho^s(t)\sigma_-. \end{aligned} \quad (19)$$

Here γ_0 is the spontaneous emission rate given by $\gamma_0 = 4\omega^3|\mathbf{d}|^2/3\hbar c^3$, and σ_+, σ_- are the standard raising and lowering operators, respectively given by

$$\sigma_+ = |1\rangle\langle 0| = \frac{1}{2}(\sigma_1 + i\sigma_2); \quad \sigma_- = |0\rangle\langle 1| = \frac{1}{2}(\sigma_1 - i\sigma_2). \tag{20}$$

Equation (19) may be expressed in a manifestly Lindblad form as

$$\frac{d}{dt}\rho^s(t) = \sum_{j=1}^{2}\left(2R_j\rho^s R_j^\dagger - R_j^\dagger R_j\rho^s - \rho^s R_j^\dagger R_j\right), \tag{21}$$

where $R_1 = (\gamma_0(N_{\rm th}+1)/2)^{1/2}R$, $R_2 = (\gamma_0 N_{\rm th}/2)^{1/2}R^\dagger$ and $R = \sigma_-\cosh(r) + e^{i\Phi}\sigma_+\sinh(r)$. This observation guarantees that the evolution of the density operator can be given a Kraus or operator-sum representation [31], a point we return to later below. If $T = 0$, then R_2 vanishes, and a single Lindblad operator suffices to describe equation (19).

In the above equation we use the nomenclature $|1\rangle$ for the upper state and $|0\rangle$ for the lower state and $\sigma_1, \sigma_2, \sigma_3$ are the standard Pauli matrices. In equation (19)

$$\begin{aligned} N &= N_{\rm th}(\cosh^2(r) + \sinh^2(r)) + \sinh^2(r), \\ M &= -\frac{1}{2}\sinh(2r)e^{i\Phi}(2N_{\rm th}+1), \\ N_{\rm th} &= \frac{1}{e^{\frac{\hbar\omega}{k_B T}} - 1}. \end{aligned} \tag{22}$$

Here $N_{\rm th}$ is the Planck distribution giving the number of thermal photons at the frequency ω and r, Φ are squeezing parameters. The analogous case of a thermal bath without squeezing can be obtained from the above expressions by setting these squeezing parameters to zero. We solve equation (19) using the Bloch vector formalism to obtain the reduced density matrix of the system in the Schrödinger picture as [43]

$$\rho^s(t) = \begin{pmatrix} \frac{1}{2}(1+A) & Be^{-i\omega t} \\ B^* e^{i\omega t} & \frac{1}{2}(1-A) \end{pmatrix}, \tag{23}$$

where,

$$\begin{aligned} A \equiv \langle\sigma_3(t)\rangle &= e^{-\gamma_0(2N+1)t}\langle\sigma_3(0)\rangle \\ &\quad - \frac{1}{(2N+1)}\left(1 - e^{-\gamma_0(2N+1)t}\right), \end{aligned} \tag{24}$$

$$\begin{aligned} B &= \left[1 + \frac{1}{2}\left(e^{\gamma_0 at} - 1\right)\right] e^{-\frac{\gamma_0}{2}(2N+1+a)t}\langle\sigma_-(0)\rangle \\ &\quad + \sinh\left(\frac{\gamma_0 at}{2}\right)e^{i\Phi - \frac{\gamma_0}{2}(2N+1)t}\langle\sigma_+(0)\rangle. \end{aligned} \tag{25}$$

Here $a = \sinh(2r)(2N_{\rm th}+1)$. Making use of equation (20), equation (25) can be written as $B = Re^{-i\chi}$. The explicit expressions for R and χ may be found in reference [43]. For the determination of GP we need the eigenvalues and eigenvectors of equation (23). The eigenvalues are

$$\lambda_\pm(t) = \frac{1}{2}(1 + \epsilon_\pm), \tag{26}$$

where $\epsilon_\pm = \pm\sqrt{A^2 + 4R^2}$. As can be seen from the above expressions, at $t = 0$, $\lambda_+(0) = 1$ and $\lambda_-(0) = 0$, hence for the purpose of GP we need only the eigenvalue $\lambda_+(t)$, and its corresponding normalized eigenvector is given as

$$|\Psi_+(t)\rangle = \sin\left(\frac{\theta_t}{2}\right)|1\rangle + e^{i(\chi(t)+\omega t)}\cos\left(\frac{\theta_t}{2}\right)|0\rangle, \tag{27}$$

where $\sin(\theta_t/2) = \frac{2R}{\sqrt{4R^2+(\epsilon_+-A)^2}} = \sqrt{\frac{\epsilon_++A}{2\epsilon_+}}$. It can be seen that for $t = 0$, $\chi(0) = \phi_0$, $\sin\left(\frac{\theta_t}{2}\right) = \sqrt{\frac{1+\langle\sigma_3(0)\rangle}{2}} \equiv \cos\left(\frac{\theta_0}{2}\right)$ and $\cos\left(\frac{\theta_t}{2}\right) = \sqrt{\frac{1-\langle\sigma_3(0)\rangle}{2}} \equiv \sin\left(\frac{\theta_0}{2}\right)$, as expected. Now we make use of equations (26), (27) in equation (11) to obtain GP as

$$\begin{aligned} \Phi_{\rm GP} = \arg\Bigg[&\left\{\frac{1}{2}\left(1 + \sqrt{A^2(\tau) + 4R^2(\tau)}\right)\right\}^{\frac{1}{2}} \\ &\times \left\{\cos\left(\frac{\theta_0}{2}\right)\sin\left(\frac{\theta_\tau}{2}\right)\right. \\ &\left. + e^{i(\chi(\tau)-\chi(0)+\omega\tau)}\sin\left(\frac{\theta_0}{2}\right)\cos\left(\frac{\theta_\tau}{2}\right)\right\} \\ &\times e^{-i\int_0^\tau dt(\dot\chi(t)+\omega)\cos^2\left(\frac{\theta_t}{2}\right)}\Bigg]. \end{aligned} \tag{28}$$

It can be easily seen from equation (28) that if we set the influence of the environment, encapsulated here by the terms γ_0, a and Φ, to zero, we obtain for $\tau = \frac{2\pi}{\omega}$, $\Phi_{GP} = -\pi(1 - \cos(\theta_0))$, as expected, which is the standard result for the unitary evolution of an initial pure state [8, 9]. Thus we see that though equations (14), (28) represent the GP of a two-level system interacting with different kinds of S-R interactions, when the environmental effects are set to zero they yield identical results. This is a nice consistency check for these expressions.

As expected, increasing the temperature, $S-R$ coupling strength or squeezing induces a departure of GP from unitary behavior. However the interpretation is less straightforward than in the QND case. Further, introduction of squeezing complicates this pattern by disrupting the monotonicity of the GP plots, as evident from the 'humps' seen for example in Figure 3B, in comparison with those in Figure 3A.

In all cases, we find that GP vanishes at $\theta_0 = \pi$, i.e., for a system that starts in the south pole of the Bloch sphere. On the other hand, for sufficiently small γ_0, we find from Figures 3A and 3B that GP may vanish also in the case $\theta_0 = 0$. These observations may be interpreted in the Bloch vector picture, and are discussed in Section 4.2.

In contrast to the situation in a purely dephasing system, GP in a dissipative system is rather complicated, and less amenable to interpretation. The dependence of GP on temperature is depicted in Figures 4 and 5. The expected pattern of GP falling asymptotically with temperature is seen. Our results parallel those obtained in references [20,46] for the case of zero squeezing (Figs. 4A and 5A), and extend them to the case of a squeezed thermal environment. We note that the effect of squeezing is to

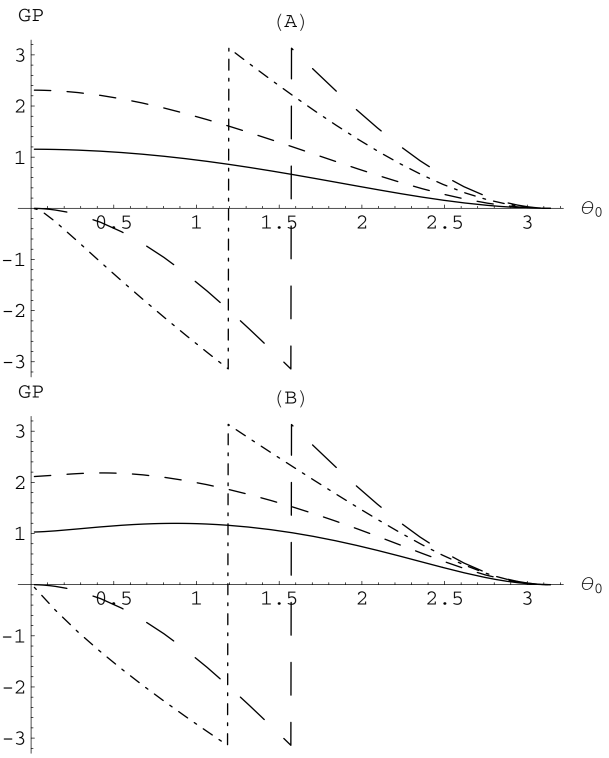

Fig. 3. GP as a function of θ_0 (in radians) for different values of γ_0 and squeezing in the Born-Markov approximation (Eq. (28)). The discontinuity in GP after π is due to the convention that an angle in the third quadrant is treated as negative. (A) $T = 0$. The large-dashed curve is the unitary case ($\gamma_0 = 0$). The dot-dashed (small-dashed) curve represents $\gamma_0 = 0.1$ ($\gamma_0 = 0.3$). The solid curve represents $\gamma_0 = 0.6$. The stationary state, for which GP vanishes, corresponds to $\theta_0 = \pi$ (i.e., $|0\rangle$), to which all states in the Bloch sphere are asymptotically driven. Thus, a qubit started in this state remains stationary and acquires no GP. (B) Same as (A), except that squeezing $r = 0.4$, $\Phi = \pi/4$.

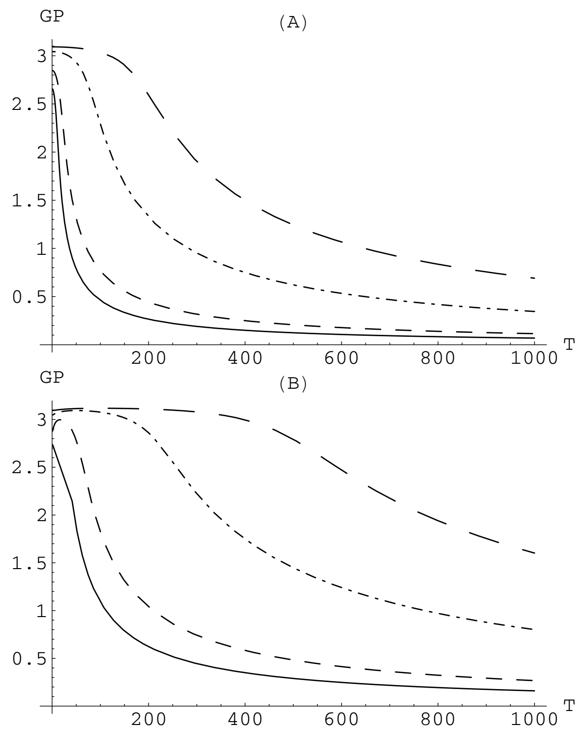

Fig. 4. GP (in radians) vs. temperature (T, in units where $\hbar \equiv k_B \equiv 1$) from equation (28). Here $\omega = 1.0$, $\theta_0 = \pi/2$, the large-dashed, dot-dashed, small-dashed and solid curves, represent, respectively, $\gamma_0 = 0.005$, 0.01, 0.03 and 0.05; (A) squeezing is set to zero, (B) squeezing non-vanishing, with $r = 0.4$ and $\Phi = 0$.

make GP vary more slowly with temperature, by broadening the peak and fattening the tails of the plots. This counteractive behavior of squeezing on the influence of temperature on GP for the case of a dissipative system is interesting, and would be of use in practical implementation of geometric phase gates. This effect can be understood by visualizing the effects of squeezing and temperature on the Bloch sphere, a point we return to in Section 4.2.

4.2 Evolution of GP in a squeezed generalized amplitude damping channel

While the results derived in this section pertain to a dissipative S-R interaction in the Born-Markov RWA, they are quite general, and are applicable to any open system effect that can be characterized as a squeezed generalized amplitude damping channel [32]. Amplitude damping channels capture the idea of energy dissipation from a system, for example, in the spontaneous emission of a photon, or when a spin system at high temperature approaches equilibrium with its environment. A simple model of an amplitude damping channel is the scattering of a photon via a beam-splitter. One of the output modes is the environment, which is traced out. The unitary transformation at the beam-splitter is given by $B = \exp\left[\theta(a^\dagger b - ab^\dagger)\right]$, where a, b and $a^\dagger, b^\dagger$ are the annihilation and creation operators for photons in the two modes. The generalized amplitude damping channel, with $T \geq 0$ and with zero squeezing, extends the amplitude damping channel to finite temperature [31]. A very general CP map generated by equation (19) has been recently obtained by us [32], and could be appropriately called the squeezed generalized amplitude damping channel. This extends the generalized amplitude damping channel by allowing for finite bath squeezing. It is characterized by the Kraus operators [32]

$$\begin{aligned}
E_0 &\equiv \sqrt{p_1}\begin{bmatrix} \sqrt{1-\alpha(t)} & 0 \\ 0 & 1 \end{bmatrix}, \\
E_1 &\equiv \sqrt{p_1}\begin{bmatrix} 0 & 0 \\ \sqrt{\alpha(t)} & 0 \end{bmatrix}, \\
E_2 &\equiv \sqrt{p_2}\begin{bmatrix} \sqrt{1-\mu(t)} & 0 \\ 0 & \sqrt{1-\nu(t)} \end{bmatrix}, \\
E_3 &\equiv \sqrt{p_2}\begin{bmatrix} 0 & \sqrt{\nu(t)} \\ \sqrt{\mu(t)}e^{-i\Phi} & 0 \end{bmatrix}.
\end{aligned} \tag{29}$$

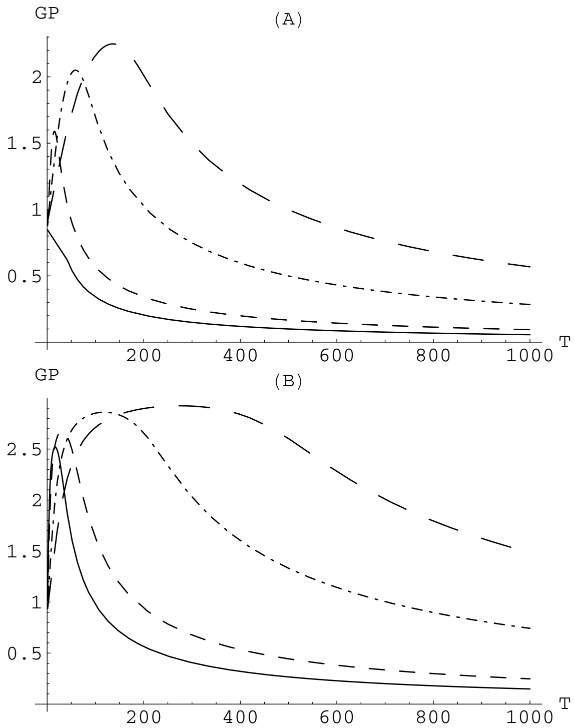

Fig. 5. GP vs. temperature (T, in units where $\hbar \equiv k_B \equiv 1$) from equation (28). Here $\omega = 1.0$, $\theta_0 = \pi/2 + \pi/4$. The curves represent $\gamma_0 = 0.005$, 0.01, 0.03 and 0.05 as in Figure 4; (A) squeezing is set to zero, (B) squeezing non-vanishing, with $r = 0.4$ and $\Phi = 0$.

With some algebraic manipulation, it can be verified that with the identification

$$
\begin{aligned}
\nu(t) &= \frac{N}{p_2(2N+1)}(1 - e^{-\gamma_0(2N+1)t}),\\
\mu(t) &= \frac{2N+1}{2p_2N}\frac{\sinh^2(\gamma_0 at/2)}{\sinh(\gamma_0(2N+1)t/2)}\\
&\quad \times \exp\left(-\frac{\gamma_0}{2}(2N+1)t\right),\\
\alpha(t) &= \frac{1}{p_1}\left(1 - p_2[\mu(t)+\nu(t)] - e^{-\gamma_0(2N+1)t}\right),
\end{aligned} \tag{30}
$$

where N is as in equation (22), the operators (29) acting on the state (9) reproduce the evolution (23), by means of the map equation (1), provided $p_2 = 1 - p_1$, satisfies

$$
\begin{aligned}
p_2 = &\frac{1}{(A+B-C-1)^2 - 4D}\\
&\times \left[A^2B + C^2 + A(B^2 - C - B(1+C) - D)\right.\\
&- (1+B)D - C(B+D-1)\\
&\pm 2\,(D(B - AB + (A-1)C + D)\\
&\left.\times\ (A - AB + (B-1)C + D))^{1/2}\right],
\end{aligned} \tag{31}
$$

where

$$
\begin{aligned}
A &= \frac{2N+1}{2N}\frac{\sinh^2(\gamma_0 at/2)}{\sinh(\gamma_0(2N+1)t/2)}\exp\left(-\gamma_0(2N+1)t/2\right),\\
B &= \frac{N}{2N+1}(1 - \exp(-\gamma_0(2N+1)t)),\\
C &= A + B + \exp(-\gamma_0(2N+1)t),\\
D &= \cosh^2(\gamma_0 at/2)\exp(-\gamma_0(2N+1)t).
\end{aligned} \tag{32}
$$

As the interaction in the Born-Markov RWA realizes a squeezed generalized amplitude damping channel [32], the various qualitative features of GP seen under a dissipative interaction (for example, the relatively complicated dependence of GP on θ_0, and on evolution time) carry over to any squeezed generalized amplitude damping channel. If squeezing parameter r is set to zero, it can be seen from above that equation (29) reduces to a generalized amplitude damping channel, with $\nu(t) = \alpha(t)$, $\mu(t) = 0$ and p_1 and p_2 being time-independent. If further $T = 0$, it can be seen from above that $p_2 = 0$, reducing equation (29) to two Kraus operators, corresponding to an amplitude damping channel.

References [11,12] consider GP evolving under an amplitude damping channel and a squeezed amplitude damping channel, respectively. These are subsumed under the squeezed generalized amplitude damping channel considered above. This channel is contractive, in that the system is seen to evolve towards a fixed asymptotic point in the Bloch sphere, which in general is not a pure state, but the mixture

$$
\rho_{\text{asymp}} = \begin{pmatrix} 1-q & 0 \\ 0 & q \end{pmatrix}, \tag{33}
$$

where $q = (N+1)/(2N+1)$. If $T = r = 0$, then $q = 1$, and the asymptotic state is the pure state $|0\rangle$. Physically this can be understood as a system going to its ground state by equilibrating with a vacuum bath, This can have a practical application in quantum computation in the form of a quantum deleter [47]. At $T = \infty$, $p = 1/2$, and the system tends to a maximally mixed state, thereby realizing a fully depolarizing channel [31].

As in the case of the QND interaction, abstracting the effect of dissipative interaction into the Kraus representation allows us to subsume all the details of the system into a limited number of channel parameters $p_1(t)$, Φ, $\alpha(t)$, $\mu(t)$ and $\nu(t)$. Any other dissipative system that can be described by a Lindblad-type master equation (19) will show a similar pattern in behavior.

To develop physical insight into the solution, we transform to the interaction picture, and for simplicity, set the squeezing parameters to zero. Then, the action of the operators (29), [which now represents a generalized amplitude channel] on an arbitrary qubit state is given in the Bloch vector representation by

$$
\begin{aligned}
\langle\sigma(t)\rangle = (&\langle\sigma_1(0)\rangle\sqrt{1-\lambda(t)}, \langle\sigma_2(0)\rangle\sqrt{1-\lambda(t)},\\
&\lambda(t)(1-2p) + \langle\sigma_3(0)\rangle(1-\lambda(t))),
\end{aligned} \tag{34}
$$

where $p = (N_{\text{th}}+1)/(2N_{\text{th}}+1)$ and $\lambda(t=\infty) = 1$. Thus, the Bloch sphere contracts towards the asymptotic mixed

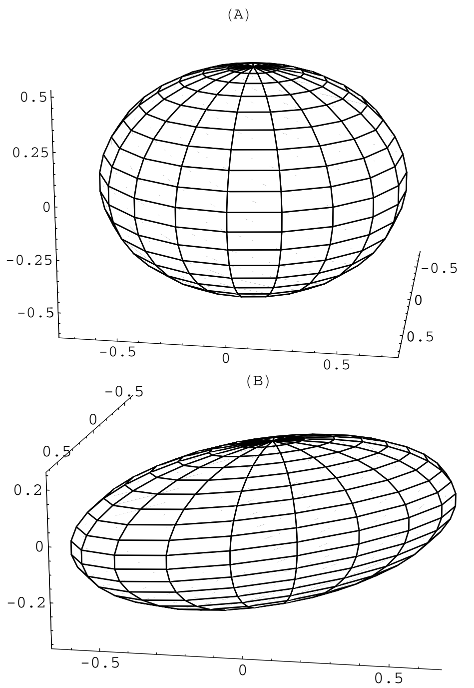

Fig. 6. Shrinking of the full Bloch sphere into an oblate spheroid under evolution given by a Born-Markov type of dissipative interaction with $\gamma_0 = 0.6$ and temperature $T = 5.0$. In (B), the x-y axes are interchanged for convenience. (A) $r = \Phi = 0$, $t = 0.15$; (B) $r = 0.4, \Phi = 1.5$, $t = 0.15$. Finite Φ is responsible for the tilt.

state $(0, 0, 1-2p)$ (Fig. 6A), characteristic of a generalized amplitude damping channel, with $T \geq 0$ and no squeezing. If $T = 0$ case, then $p = 1$, and the asymptotic state $(0, 0, -1)$ is pure.

The Bloch vector picture allows us to interpret the results of Section 4.1. Equations (23), show that the Bloch vector for the states corresponding to $\theta_0 = 0, \pi$ move only along the z-axis of the Bloch sphere for zero as well as finite T. For the case $\theta_0 = \pi$ and zero T, the Bloch vector remains stationary at $(0, 0, -1)$, and hence GP vanishes. In the finite T case, GP still vanishes, because the Bloch vector has the form $(0, 0, -L(t))$, where the Bloch vector length $L(t)$ shrinks from 1 towards an interaction-dependent asymptotic value, which is zero for infinite temperature or finite otherwise. Since the Bloch vector shrinks strictly along its length, and thus subtends no finite angle at the center of the sphere, we find that GP vanishes at $\theta_0 = \pi$, as expected (cf. Figs. 3).

On the other hand, even though the Bloch vector shrinks similarly along its length in the case $\theta_0 = 0$, we find that GP is non-vanishing in certain cases, in fact, in precisely those cases where the tip of the Bloch vector crosses the center of the Bloch sphere moving along the σ_3-axis. That is, they correspond to the situation where $\langle \sigma_3(t) \rangle$ changes sign from positive to negative during the period of one cycle. In these cases, the dependence of GP on the Bloch vector is too involved for us to interpret in terms of L and the angle subtended by the Bloch vector, for some qualitative insight. Nevertheless this feature may be formally understood as follows. It can be observed from equation (24) that for sufficiently large γ_0, $\langle \sigma_3(t) \rangle$ changes sign at $t_1 \equiv \log(2[N+1])/(\gamma_0[2N+1])$. Further, we note that R vanishes for $\theta_0 = 0$ (as well as $\theta_0 = \pi$).

It is convenient to recast equation (28) in the expanded form

$$\begin{aligned}\Phi_{\rm GP} = \tan^{-1} &[(\sin(\chi(\tau) - \chi(0) + 2\pi) \sin(\theta_0/2) \cos(\theta_\tau/2)) \\ &\div \{\cos(\chi(\tau) - \chi(0) + 2\pi) \sin(\theta_0/2) \cos(\theta_\tau/2) \\ &+ \cos(\theta_0/2) \sin(\theta_\tau/2)\}] \\ &- \int_0^\tau dt(\dot{\chi}(t) + \omega) \cos^2\left(\frac{\theta_t}{2}\right). \end{aligned} \tag{35}$$

It can be seen that for the case $\theta_0 = \pi$, $\cos(\theta_t/2) = 1$ and, in particular, $\cos(\theta_\tau/2) = 1$. Substituting these values in equation (35), it is seen that GP vanishes because the two terms in the RHS of equation (35) cancel each other. Next consider the case where $\theta_0 = 0$ but where γ_0 is sufficiently weak that $\tau \leq t_1$, i.e., $\langle \sigma_3(t) \rangle$ does not change sign during one cycle. In this case, from above it is seen that $\cos(\theta_t/2) = 0$, and, in particular, $\cos(\theta_\tau/2) = 0$, and thus the terms in the RHS of equation (35) vanish identically. But in the case of $\theta_0 = 0$ where $\tau > t_1$ (γ_0 being relatively stronger), $\cos(\theta_t/2) = 0$ initially in the time interval $[0, t_1]$, and then switches to 1 in the interval $(t_1, \tau]$. In particular, $\cos(\theta_\tau/2) = 1$. Observe that if $\cos(\theta_t/2) = 1$ throughout the interval $[0, \tau]$, the two terms in the RHS cancel each other. It follows that GP is non-vanishing because of an excess contributed by the first term, in the interval $[0, t_1]$.

Contraction produced by an increase in temperature tends to be less pronounced in the presence (than in the absence) of squeezing (Figs. 6). This is reflected in the slower variation of GP with respect to temperature, seen in Figures 4B and 5B in relation to Figures 4A and 5A, respectively. As observed in Figures 4 and 5, GP falls as a function of T, for sufficiently large T. This may quite generally be attributed to the reduction in L and Ω caused by the contraction of Bloch vector as a result of interaction with the environment. The tilt of the contracted Bloch sphere in Figure 6B is due to finite Φ.

5 Conclusions

We have studied the combined influence of squeezing and temperature on the GP for a qubit interacting with a bath both in a non-dissipative as well as in a dissipative manner. In the former case, squeezing has a similar debilitating effect as temperature on GP. In contrast, in the latter case, squeezing can counteract the effect of temperature in some regimes. This makes squeezing potentially helpful for geometric quantum information processing and geometric computation. In particular, in the context of using engineered (e.g., squeezed) reservoirs to generate GP [29], it would be helpful to consider the effect of squeezing together with thermal effects [20,21].

In the non-dissipative (QND) case, we analyzed a number of open system models using two types of bath: the usual one of harmonic oscillators, and that of two-level systems. It was shown that for the case of weak $S-R$ coupling, the two kinds of baths can be mapped onto each other. GP was studied as a function of the initial polar angle θ_0 of the Bloch sphere, temperature and squeezing (arising from the squeezed thermal bath). In the QND case, it was seen that increasing γ_0, temperature or squeezing tends to cause a similar departure from unitary behavior by suppressing GP.

However, in the dissipative case (with the environment modelled as a squeezed thermal bath in the weak Born-Markov RWA), we found that the dependence of GP on θ_0, temperature and squeezing shows a greater complexity. Here, an interesting feature due to squeezing is that it can disrupt, over an interval, the otherwise monotonic behavior of GP as a function of θ_0 (the humps seen in Fig. 3B). More pronouncedly, the counteractive effect of squeezing on temperature is brought out by a comparison of Figures 4A with 4B, and 5A with 5B. Also, its effect on the Bloch sphere is to shrink it to an oblate spheroid, in contrast to a QND interaction, which produces a prolate spheroid. Thus, an interesting feature that emerges from our work is the contrast in the interplay between squeezing and thermal effects in non-dissipative and dissipative interactions. By interpreting the open quantum effects as noisy channels, we make the connection between geometric phase and quantum noise processes familiar from quantum information theory.

An added feature of our work is that we make a connection between the studied open system models and the phase damping and the newly introduced squeezed generalized amplitude damping [32] channels, noise processes which are important from a quantum information theory perspective. In particular, we give a detailed microscopic basis for these noisy channels. This allows us to study the effects of the formal noise processes on GP.

References

1. S. Pancharatnam, Proc. Ind. Acad. Sci. A **44**, 247 (1956)
2. M.V. Berry, Proc. R. Soc. Lond. A **392**, 45 (1984)
3. B. Simon, Phys. Rev. Lett. **51**, 2167 (1983)
4. Y. Aharonov, J. Anandan, Phys. Rev. Lett. **58**, 1593 (1987)
5. J. Samuel, R. Bhandari, Phys. Rev. Lett. **60**, 2339 (1988)
6. N. Mukunda, R. Simon, Ann. Phys. (N.Y.) **228**, 205 (1993)
7. A. Uhlmann, Rep. Math. Phys. **24**, 229 (1986); Ann. Phys. **46**, 63 (1989); A. Uhlmann, Lett. Math. Phys. **21**, 229 (1991)
8. E. Sjöqvist et al., Phys. Rev. Lett. **85**, 2845 (2000)
9. K. Singh et al., Phys. Rev. A **67**, 032106 (2003)
10. D.M. Tong, E. Sjöqvist, L.C. Kwek, C.H. Oh, Phys. Rev. Lett. **93**, 080405 (2004)
11. Z.S. Wang, L.C. Kwek, C.H. Lai, C.H. Oh, Europhys. Lett. **74**, 958 (2006)
12. Z.S. Wang et al., Phys. Rev. A **75**, 024102 (2007)
13. M.-M. Duan, I. Cirac, P. Zoller, Science **292**, 1695 (2001)
14. R. Balakrishna, M. Mehta, Eur. Phys. J. D **33**, 437 (2005)
15. G. Falci, R. Fazio, G.H. Palma, J. Siewert, V. Vedral, Nature **407**, 355 (2000)
16. J.A. Jones, V. Vedral, A. Ekert, G. Castagnoli, Nature **403**, 869 (2000)
17. Y. Nakamura, Yu. A. Pashkin, J.S. Tsai, Nature **398**, 786 (1999)
18. R.S. Whitney, Y. Gefen, Phys. Rev. Lett. **90**, 190402 (2003); R.S. Whitney, Y. Makhlin, A. Shnirman, Y. Gefen, Phys. Rev. Lett. **94**, 070407 (2005)
19. G. De Chiara, A. Lozinski, G.M. Palma, e-print `arXiv:quant-ph/0410183`
20. A.T. Rezakhani, P. Zanardi, Phys. Rev. A **73**, 052117 (2006)
21. F.C. Lombardo, P.I. Villar, Phys. Rev. A **74**, 042311 (2006)
22. M.S. Sarandy, D.A. Lidar, Phys. Rev. A **73**, 062101 (2006)
23. X.X. Yi, D.P. Liu, W. Wang, New J. Phys. **7**, 222 (2005)
24. X.X. Yi, L.C. Wang, W. Wang, Phys. Rev. A **71**, 044101 (2005)
25. X.X. Yi et al., Phys. Rev. A **73**, 052103 (2006)
26. T.A.B. Kennedy, D.F. Walls, Phys. Rev. A **37**, 152 (1988)
27. M.S. Kim, V. Bužek, Phys. Rev. A **47**, 610 (1993)
28. S. Banerjee, R. Ghosh, e-print `arXiv:quant-ph/0703054`
29. A. Carollo et al., Phys. Rev. Lett. **96**, 150403 (2006)
30. K. Kraus, *States, Effects and Operations* (Springer-Verlag, Berlin, 1983)
31. M. Nielsen, I. Chuang, *Quantum Computation and Quantum Information* (Cambridge University Press, Cambridge, 2000)
32. R. Srikanth, S. Banerjee, e-print `arXiv:0707.0059`
33. W.G. Unruh, Phys. Rev. A **51**, 992 (1995)
34. G.M. Palma, K.-A. Suominen, A.K. Ekert, Proc. R. Soc. Lond. A **452**, 567 (1996)
35. D.P. DiVincenzo, Phys. Rev. A **51**, 1015 (1995)
36. C.M. Caves, B.L. Schumacher, Phys. Rev. A **31**, 3068 (1985); B.L. Schumacher, C.M. Caves, Phys. Rev. A **31**, 3093 (1985)
37. R.H. Dicke, Phys. Rev. **93**, 99 (1954)
38. J.M. Radcliffe, J. Phys. A: Gen. Phys. **4**, 313 (1971)
39. F.T. Arecchi, E. Courtens, R. Gilmore, H. Thomas, Phys. Rev. A **6**, 2211 (1972)
40. J. Shao, M.-L. Ge, H. Cheng, Phys. Rev. E **53**, 1243 (1996)
41. J. Shao, P. Hänggi, Phys. Rev. Lett. **81**, 5710 (1998)
42. N.V. Prokof'ev, P.C.E. Stamp, Rep. Prog. Phys. **63**, 669 (2000)
43. S. Banerjee, R. Srikanth, e-print `arXiv:quant-ph/0611161`
44. M.O. Scully, M.S. Zubairy, *Quantum Optics* (Cambridge University Press, Cambridge, 1997)
45. H.-P. Breuer, F. Petruccione, *The Theory of Open Quantum Systems* (Oxford University Press, 2002)
46. K.-P. Marzlin, S. Ghose, B.C. Sanders, Phys. Rev. Lett. **93**, 260402 (2004)
47. R. Srikanth, S. Banerjee, Phys. Lett. A **367**, 295 (2007)